3D analytical modelling of plate fin heat sink on forced convection

A. Castelan, B. Cougo, Sébastien Dutour, Thierry Meynard

▶ **To cite this version:**

A. Castelan, B. Cougo, Sébastien Dutour, Thierry Meynard. 3D analytical modelling of plate fin heat sink on forced convection. Mathematics and Computers in Simulation, 2019, 158, pp.296-307. 10.1016/j.matcom.2018.09.011 . hal-02403664

HAL Id: hal-02403664
https://hal.science/hal-02403664

Submitted on 21 Oct 2021

HAL is a multi-disciplinary open access archive for the deposit and dissemination of scientific research documents, whether they are published or not. The documents may come from teaching and research institutions in France or abroad, or from public or private research centers.

L'archive ouverte pluridisciplinaire **HAL**, est destinée au dépôt et à la diffusion de documents scientifiques de niveau recherche, publiés ou non, émanant des établissements d'enseignement et de recherche français ou étrangers, des laboratoires publics ou privés.

Distributed under a Creative Commons Attribution - NonCommercial 4.0 International License

Version of Record: https://www.sciencedirect.com/science/article/pii/S037847541830243X
Manuscript_1e0001192459ffd18ee23f001cfa2ff0

3D ANALYTICAL MODELLING OF PLATE FIN HEAT SINK ON FORCED CONVECTION

A. CASTELAN[1,2,3], B. COUGO[1], S. DUTOUR[3], T. MEYNARD[2]

1. IRT Saint-Exupéry, 118, route de Narbonne - CS 44248, 31432 Toulouse cedex 4, France
2. LAPLACE, INP-ENSEEIHT, 2 rue Charles Camichel - BP 7122, 31071 Toulouse cedex 7, France
3. LAPLACE, Université Paul Sabatier - Bat3R3, 118 route de Narbonne, 31062 Toulouse cedex 9, France
E-mail: anne.castelan@irt-saintexupery.com

Abstract - With the development of embedded systems, it is crucial to reduce weight of equipments. In power converter, heat sink is a heavy part that often can be reduced in volume and weight. There are several models and methods to calculate a heat sink thermal resistance. However the more precise these methods are, the more time consuming they are and thus they can be hardly integrated in a weight optimization routine. Using analytical models to calculate heat sink thermal resistance is a good compromise between execution time and precision of results. They are usually one-dimensional models which are simple but do not take into account heat spreading effects, which is important when power electronic heat sources are small compared to their heat sink. This paper describes a three-dimensional analytical model of forced convection plate fin heat sink, which will be compared with numerical simulation. A maximum difference of 1.4°C has been observed between the mean ΔT of the models. This analytical model will be used in an optimization routine to reduce the weight of an existing heat sink in order to show that fast and precise optimization of cooling system is possible with analytical models.

Keywords – Heat Sink, 3D FEM Simulation, Analytical Modelling, Power Converter, Optimization.

1. INTRODUCTION

Real development of more electrical aircraft is only possible if high level of equipment integration is achieved, i.e. if one can reduce at most the system's mass and increase power density. One of the most important equipments that must be optimized is a static power converter, which can be found in many applications inside an aircraft.

Designing a power converter always implies on finding the best trade-off between cost, mass, efficiency and reliability applied to different elements such as capacitors, inductors, switches, cooling system (heat sinks), control boards and etc. Most of the times, the heat sink, which is one of the heaviest elements, is only evaluated at the end of the design process and is often oversized.

Heat sinks are generally made of aluminium and sometimes of copper and other materials. Thus, heat sink is a heavy element, which significantly contributes to the converter weight. For that reason increasing power density of a power converter implies on reducing at maximum the heat sink weight.

Moreover, since reliability is a major aspect in any aircraft application, liquid cooling heat sink should be avoided. The use of pumps and fluid circulation circuits requires regular maintenance and decreases system reliability. For that reason, it is essential to use fin heat sinks in natural or forced convection.

Weight optimization of fin heat sinks can be only achieved by the use of adapted models, which are precise enough to design a valid device but fast enough to be executed in a reasonable time. Calculation of heat sink thermal resistances and temperatures is possible either by very precise 3D Finite Element Method (FEM) simulations or by analytical models. FEM simulations are very time consuming and are hardly integrated in optimization routines. On the other hand, analytical modelling is usually fast but inaccurate. Our goal is to then develop a heat sink analytical model, which is fast enough to take part of a power converter optimization routine, and at the same time fairly precise (maximum 5% difference between analytical calculation and FEM simulation).

Modelling presented in [1] and shown in this paper concerns forced convection heat sinks with plate fins which is one of the most robust, cheap and thus common types of cooling systems. Analytical model to describe a plate fin heat sink will be developed in this paper. The goal of this model is to give the mean heat source(s) temperature(s) for any source and heat sink dimensions, source position on the heat sink baseplate, and fan associated to the heat

© 2018 published by Elsevier. This manuscript is made available under the CC BY NC user license
https://creativecommons.org/licenses/by-nc/4.0/

sink. A state of art of an existing model will be first presented before we develop the model used in our optimization routines. After that, a comparison between FEM and the developed analytical model will be shown in order to confirm that it is precise enough to be used for fast design.

Finally, this model will be integrated in an optimization routine so a thermal system design can be performed. An example of heat sink design for a power converter used in aircraft applications will be shown. This example illustrates how fast the developed optimization routines are and also the importance of taking into account heat spreading in the baseplate of the heat sink.

2. STATE OF ART OF EXISTING MODELS

There are different studies for heat sink weight reduction, however developed models are either very simple (proportional relation between weight and thermal resistance, often used for predesigning components), or very complex (using FEM software).

Analytical models of different forms used to describe heat sink with plate fins, in forced or natural convection, are found in literature. These models are most of the time resistive models, and are generally based on one-dimensional approximations [2, 3, 4]. The main advantage of these models is that they are easy to employ since they are similar to electrical models. These models have been tested for Biot number of 1, for several case of dimensionless number corresponding to the ratio of normalized area of the hot spot to the normalized area of the base plate (0.005 to 0.125).

There are also two or three-dimensional models, coming from direct resolution of heat transfer equations and that are then more precise models [5, 6, 7, 8, 9, 10, 11]. The main advantage of these 2D/3D models is that they consider more realistic propagation effects of the heat produced by the heat source (usually power components). Power components are usually smaller than the heat sink baseplate and like so there is a real spreading effect of the heat in this baseplate. This spreading phenomenon is not easily and precisely described with resistive models based on one-dimensional approximations. These models are dedicated to semi-infinite and finite mean [7,8,9,10,11]. For the models in [5,6], fixed geometrical configurations are tested for several air flow (until 14 dm^3/s).

For that reason, the approach proposed in this work combines the general 3D description of heat spreading as shown in [11] and a fin model to obtain an analytical description of the whole thermal component. Thus, many different configurations, size and position of heat sources and heat sink can be considered.

3. HEAT SINK MODEL

Heat sink and fan models are based on geometrical parameters shown in Fig. 1. These parameters are the fin height H_{FIN}, the baseplate thickness H_{BP}, the length L and width W of the heat sink, the space between fins b, corresponding to the channel where air is pulsed by the fan, the fin thickness T_{FIN} and the number of fins n_{FIN}.

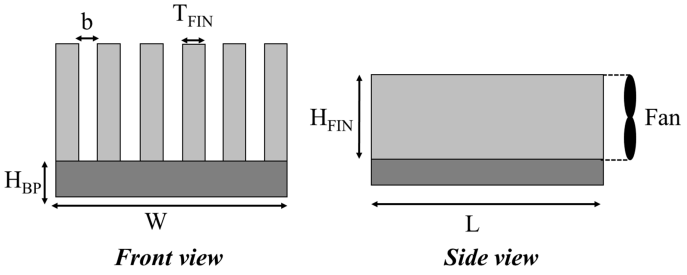

Fig. 1: Geometrical parameters of extruded heat sink and fan.

Heat sink design procedure is schematically shown in Fig. 2. Inputs of this procedure are: number, size, location and power of heat sources; heat sink geometry (number of fins, geometrical dimensions); heat sink material; and fan characteristics. Outputs (results) are the values of the average temperature of each heat source, as well as the weight value of the cooling system (heat sink + fan). Note that a thermal resistance R_{TH} of the cooling system can be calculated in the case of only one heat source connected to the heat sink.

Different constraints can be added to the design procedure such as the maximum and minimum values of geometrical parameters or the maximum temperature of heat sources.

Blocs 1 to 3 of Fig. 2 concern the choice of heat sink geometrical parameters and fan, the determination of fan operation point (based on the calculation of static pressure drop of the heat sink) and the calculation of the equivalent fin thermal resistance which is determined based on the aeraulic model applied to the fins. This model

is established by a Nusselt number correlation. Details on this calculation are given in [12] and will not be presented here.

Instead, this paper explains in details Bloc 4 and Bloc 5. In these blocs, thermal resistance values calculated for each fin (R_{TH_FIN}) is used to calculate an equivalent heat transfer coefficient (h_{EQ}) which will be applied to the entire bottom surface of the heat sink baseplate. In this way, heat spreading can be calculated in Bloc 6 with model of [11], which gives a 3D model of the baseplate. In Bloc 7, temperature, thermal resistance and weight of the designed heat sink are calculated and results are found.

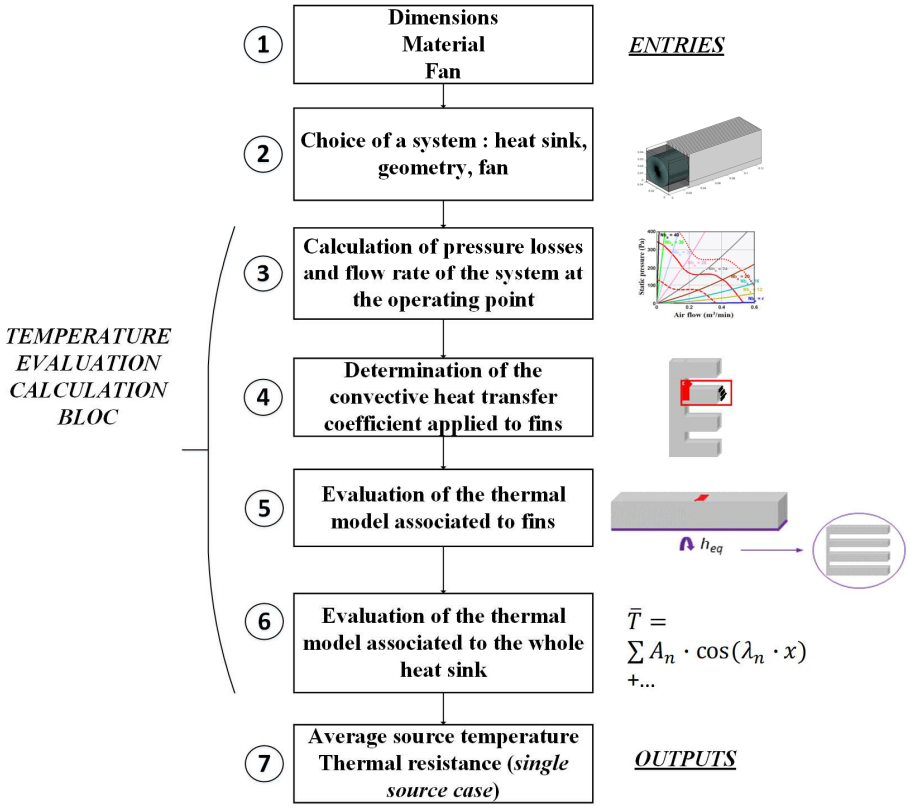

Fig. 2: Design procedure to optimize the weight of cooling system composed of heat sink and fan.

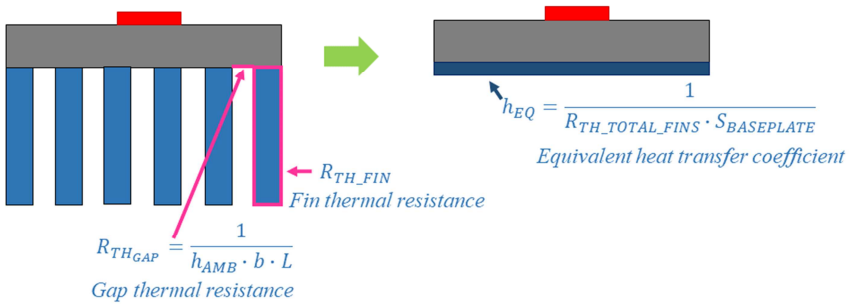

Fig. 3: Equivalence between fin thermal resistance (R_{TH_FIN}) and heat exchange coefficient (h_{EQ}) used to calculate heat spreading in heat sink baseplates

3.1. BASEPLATE MODEL

This equivalent heat transfer coefficient h_{EQ} between the lower surface of the base plate $S_{BASEPLATE}$ and the ambient is determined from the thermal resistance of fins and gap between fins as illustrated in Fig. 3 and as defined in (1).

$$h_{EQ} = \frac{1}{R_{TH\_TOTAL\_FINS} \cdot S_{BASEPLATE}} \quad (1)$$

where $R_{TH\_TOTAL\_FINS}$ accounts for all the thermal transfer existing in the fins, i.e. conduction along the fins and convective transfer with the ambient air. The contribution of the fin itself and the gap between two fins is considered in the definition of $R_{TH\_TOTAL\_FINS}$, as shown in (2).

$$\frac{1}{R_{TH\_TOTAL\_FINS}} = \frac{N_{FINS}}{R_{TH\_FIN}} + h_{AMB} \cdot b \cdot L \cdot (N_{FINS} - 1) \quad (2)$$

where h_{AMB} is the convective coefficient applied to fin surface and given by the aeraulic model and the Nusselt correlation. R_{TH_FIN} is the thermal resistance of one single fin, given by (3), where S_{FIN} is the cross section of the fin ($T_{FIN} \bullet L$), λ_{FIN} is the fin conductivity and α is given by (4).

$$R_{TH\_FIN} = \frac{1}{\alpha \cdot \lambda_{FIN} \cdot S_{FIN} \cdot \tanh(\alpha \cdot H_{FIN})} \quad (3)$$

$$\alpha = \sqrt{\frac{h_{AMB} \cdot 2 \cdot (T_{FIN} + L)}{\lambda_{FIN} \cdot S_{FIN}}} \quad (4)$$

The aeraulic correlation comes from [13], and gives a mean convective heat transfer coefficient in the fin section. This correlation, associated with a pressure drop model usually used in literature [14] gives good correlation of the thermal behavior of a heat sink in air forced convection, as it can be seen in section 4.

This equivalent heat transfer coefficient h_{EQ} gives the information about the thermal behavior of the fins. It is an entry value for the baseplate thermal model. The approach proposed in this paper, which associates the fin model and the base plate model, is new and it is more accurate than 1D approaches where the 1D thermal models of base plate and fins are associated as thermal resistances connected in series. The 1D approach considers the hypothesis of a uniform temperature at the bottom of the baseplate and like this all the fins present the same temperature at their connection with the base plate. This is not a good approach in real systems where the heat source is smaller than the base plate and the temperature at the bottom of the baseplate is not uniform. The equivalent transfer coefficient h_{EQ} presented in this paper avoids the uniform temperature hypothesis and thus the link between the fin model and the baseplate model is more realistic.

Then, solving the heat diffusion in the baseplate [11], it is possible to determine the mean temperature of the heat source, whatever its position is, with the relation:

$$\begin{aligned}\overline{\Delta T} = \overline{T}_{SOURCE} - T_{AMB} = \overline{\Delta T}_{1D} + 2 \cdot \sum_{m=1}^{\infty} A_m \cdot \frac{\cos(\lambda_m \cdot X_c) \cdot \sin(0.5 \cdot \lambda_m \cdot c)}{\lambda_m \cdot c} \\ + 2 \cdot \sum_{n=1}^{\infty} A_n \cdot \frac{\cos(\delta_n \cdot Y_c) \cdot \sin(0.5 \cdot \delta_n \cdot d)}{\delta_n \cdot d} + 4 \cdot \left(\sum_{m=1}^{\infty} \sum_{n=1}^{\infty} A_{m,n} \cdot \frac{\cos(\delta_n \cdot Y_c) \cdot \sin(0.5 \cdot \delta_n \cdot d)}{\lambda_m \cdot c \cdot \delta_n \cdot d} \cdot \cos(\lambda_m \cdot X_c) \cdot \sin(0.5 \cdot \lambda_m \cdot c) \right)\end{aligned} \quad (5)$$

where $\overline{\Delta T}$ is the mean temperature rise of the heat source when compared to ambient temperature and

$$\overline{\Delta T}_{1D} = \frac{Q}{W \cdot L} \cdot \left(\frac{H_{BP}}{\lambda} + \frac{1}{h_{EQ}} \right) \quad (6)$$

Fourier coefficients A_m, A_n, A_{mn} are given in [11] and depend on the source dimensions, the power evacuated, the source position on the baseplate, the dimensions of the baseplate and the heat transfer coefficient applied on the bottom of the baseplate. Complete details of these expressions are shown in [11]. λ_m, δ_n, β_{mn}, are the eigenvalues of each part of the solution. Parameters c and d correspond to the width and the length of the heat source; X_C and Y_C are the coordinates of the heat source center point referred to a baseplate corner. Q is the power dissipated by the source, a and b are the width and the length of the baseplate, H_{BP} is the baseplate thickness, λ is the baseplate conductivity, and h_{EQ} is the heat transfer coefficient of (1).

The analytical relation of (5) is obtained by solving the heat equation, in steady state, and in three dimensions, given in (7). The material is supposed to have homogeneous properties in all directions. These properties (conductivity….) are independent of the temperature variation and are considered constant.

$$\frac{\partial^2 T(x,y,z)}{\partial x^2} + \frac{\partial^2 T(x,y,z)}{\partial y^2} + \frac{\partial^2 T(x,y,z)}{\partial z^2} = 0 \quad (7)$$

As shown in [11], in a system with *Ns* heat sources, superposition can be applied to calculate the mean temperature rise of each heat source. For that, one must take into account the influence of all heat sources in order to calculate the mean temperature rise in one heat source. This can be calculated, for a certain heat source "*j*" as:

$$\overline{T}_{SOURCE\ j} - T_{AMB} = \sum_{i=1}^{Ns} \overline{\Delta T}_i \qquad (8)$$

Where $\overline{T}_{SOURCE\ j}$ is the mean temperature of source "*j*", T_{AMB} is the temperature of the air around the heat sink, and $\overline{\Delta T}_i$ is the mean temperature rise contribution of all sources, calculated at the coordinates of the source "*j*". It means that $\overline{\Delta T}_i$ has the same analytical expression as (5) for a single source, however Fourier coefficients are evaluated at the source "*i*", but the temperature expression is evaluated at the source "*j*" coordinates and dimensions. The complete details of these expressions are also described in [11].

4. NUMERICAL COMPARISON

Once this analytical model is established, it is necessary to quantify the difference of results using this analytical model and a precise 3D numerical simulation with finite element methods (FEM). This numerical comparison of the analytical model is performed using COMSOL software.

A complete heat sink (baseplate and fins) has been realized as shown in Fig. 4 for a given dimension of heat sink and heat source. Same dimensions and heat source have been used in both models (analytical and FEM simulation).

Heat sink has 17 fins of 6.1mm thickness and 40mm height. Baseplate has dimensions: thickness H_{BP}=0.009m, length *L*=0.1m and width *W*=0.2m. The square heat source is centered, and has initially width and length (respectively *c* and *d*) of 0.02m and it dissipates 100W. Width and length of the heat source will vary during the study. The convective heat transfer uniformly applied on fins is 50 W/m²K in order to simulate a wind speed of approximately 1m/s. The choice of using this uniform convective heat transfer coefficient is related to the fin thermal model we used since the aeraulic model gives an average coefficient along the fins.

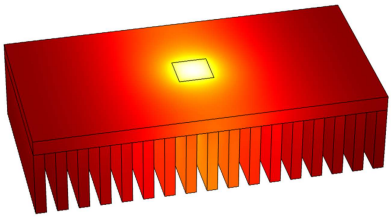

Fig. 4: Example of simulation result of heat sink with plate fins in forced convection used to compare with the developed analytical model.

For different ratio of heat source dimensions and baseplate dimensions, a maximum difference of 1.4°C (corresponding to 2.5% of temperature rise) has been observed in the calculation of the heat source mean temperature rise between analytical and numerical models. This difference of temperature is given in (9).

$$\varepsilon = \overline{\Delta T}_{ANALYTIC} - \overline{\Delta T}_{COMSOL} \text{ or } \varepsilon = \frac{\overline{\Delta T}_{ANALYTIC} - \overline{\Delta T}_{COMSOL}}{\overline{\Delta T}_{ANALYTIC}} \cdot 100\,\% \qquad (9)$$

Where

$$\overline{\Delta T}_{ANALYTIC} = \overline{T}_{SOURCE} - T_{AMB}$$

This difference is shown in Fig. 5 where the dimensions of the heat source is changed so its surface is varied from 5% to 50% of the baseplate surface. As it can be seen in this figure, when the heat source size increases, this difference decreases. The increase of surface reduces the spreading effect and brings the configuration close to a one-dimensional conduction case in the base plate.

Although Fig. 5 shows an example using a single heat source, low difference between the two models is also observed when several sources are simulated on the baseplate.

The use of analytical model gives results almost as precise as finite element method model, on simple configurations. However, analytical model execution is very fast compared to numerical model. In this specific example, the resolution of a numerical model took about 15 minutes in a dual-core Intel Xeon, 3.2GHz having 64GB of RAM memory; and about 5.5ms for the analytical calculation in a Personal Computer having an Intel Core i7, 1.8GHz and 8GB of RAM memory.

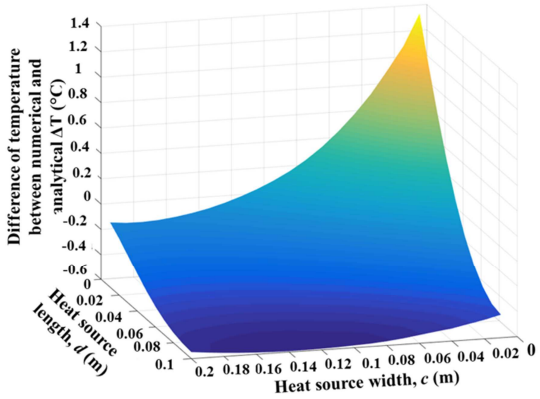

Fig. 5: Difference between the heat source mean temperature rise evaluation using the proposed analytical model and a 3D FEM simulation for different heat source dimensions.

5. OPTIMIZATION OF THE HEAT SINK

Using the proposed analytical model in a optimization routine is certainly interesting because this model has a very fast calculation and also considers heat spreading in the baseplate of a heat sink, which is not the case of models in [5,6]. The baseplate is, in several heat sink designs, the heaviest part of the heat sink. Thus, having a precise model of heat spreading in this baseplate will help reducing the weight and then improving the integration of the heat sink into the power converter.

In order to illustrate the influence of the baseplate in the heat sink thermal resistance and also the use of the proposed models in the optimization of a heat sink, an example is given below. A three-phase power inverter for aircraft applications using a SiC power module (reference CCS050M12CM2, from manufacturer CREE) of nominal power of 15kW is used as reference. Losses at this power module are dissipated in a high performance forced air-cooling system of reference LA6-150, from manufacturer FischerElektronik, which will be consider as the reference design. This cooling system has thermal resistance of 0.175K/W at maximum fan power. Note that this thermal resistance value is given for a heat source of the same size as the heat sink baseplate. Fan weight is 0.066kg and the aluminium heat sink weight is 0.830kg. Dimensions of heat sink and heat source (power module) are given in Fig. 6.

In a first example, the influence of the baseplate in the total thermal resistance will be shown. A heat sink with 30 fins of 26.6mm height, a baseplate of 50.6mm width, 150mm length and a baseplate thickness varying from 3 to 20mm is considered. The heat source is the power module, having dimensions of 47mm width and 108mm long. Calculation of thermal resistance of the heat sink using the proposed heat spreading model (3D model) and using a 1D model is shown in Fig. 7 for the baseplate thickness variation. It can be seen that, when baseplate thickness increases, heat sink thermal resistance decreases up to a minimum point and then it increases using the 3D model while it always increases using the 1D model. The difference between the maximum and minimum thermal resistance using the 3D is not that high given that the surface of the heat source is close to that of the baseplate. For the same reason, the difference between the 3D and 1D models is not so high (about 8% at thickness of 3mm, calculated with the relation from (9)). Obviously, this different could be much higher for heat sources with smaller surface. In Fig. 7 we illustrate a thermal behaviour of a configuration where heat source surface is 72% of the base plate surface.

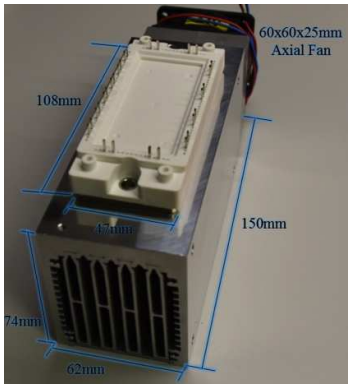

Fig. 6: Heat sink, fan and power module used as reference in the example of heat sink optimization.

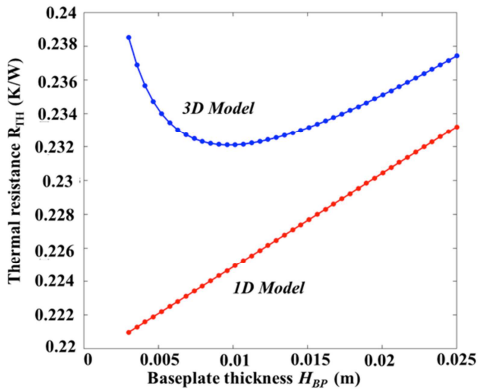

Fig. 7: Variation of the global thermal resistance of a heat sink with the baseplate thickness using 1D and 3D models. Since the heat source surface is close to that of the heat sink baseplate, 3D effect is not so high and both 1D and 3D models have similar results.

If the heat source is smaller than the base plate surface, for example if the heat source surface is 20% of the base plate surface, the influence of spreading effect on thermal performances is more important, as can be seen in Fig. 8. In this example, the evolution of thermal resistances has the same form of that of Fig. 7. However the differences between 1D and 3D models is more significant. When the base plate is very thin (3mm), the difference of thermal resistance between models is 19.5%. This difference is calculated from (10)

$$\varepsilon_{R_{TH}} = \frac{R_{TH\_3D} - R_{TH\_1D}}{R_{TH\_3D}} \cdot 100\ \% \qquad (10)$$

Even when the base plate thickness increases, the difference between models is more important than previously. When base plate is thick (25mm), the difference of thermal resistance between models is 7%, when compared to 1.5% for a heat source surface equals to 72% of the base plate surface. In such cases, it is then really important to consider a 3D model to accurately design a heat sink.

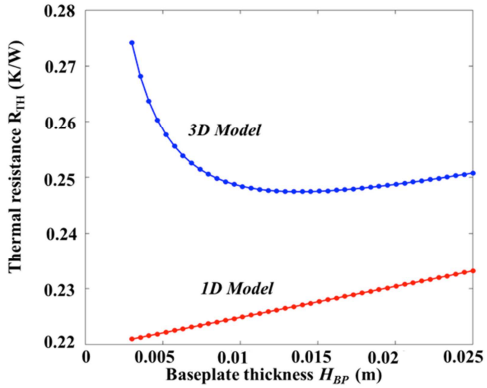

Fig. 8: Variation of the global thermal resistance of a heat sink with the baseplate thickness using 1D and 3D models. As heat source is significantly smaller than the heat source, about 20%, the 3D effect is significant.

In the second example, the analytical model is coded in MATLAB and used in an optimization routine based on parametrical variation of 6 parameters. The algorithm used is illustrated in Fig. 9. The fan characteristic is the same as the one for the first example. Since the analytical model is very fast to compute, many points for each parameter can be calculated and no deterministic optimization technique is needed.

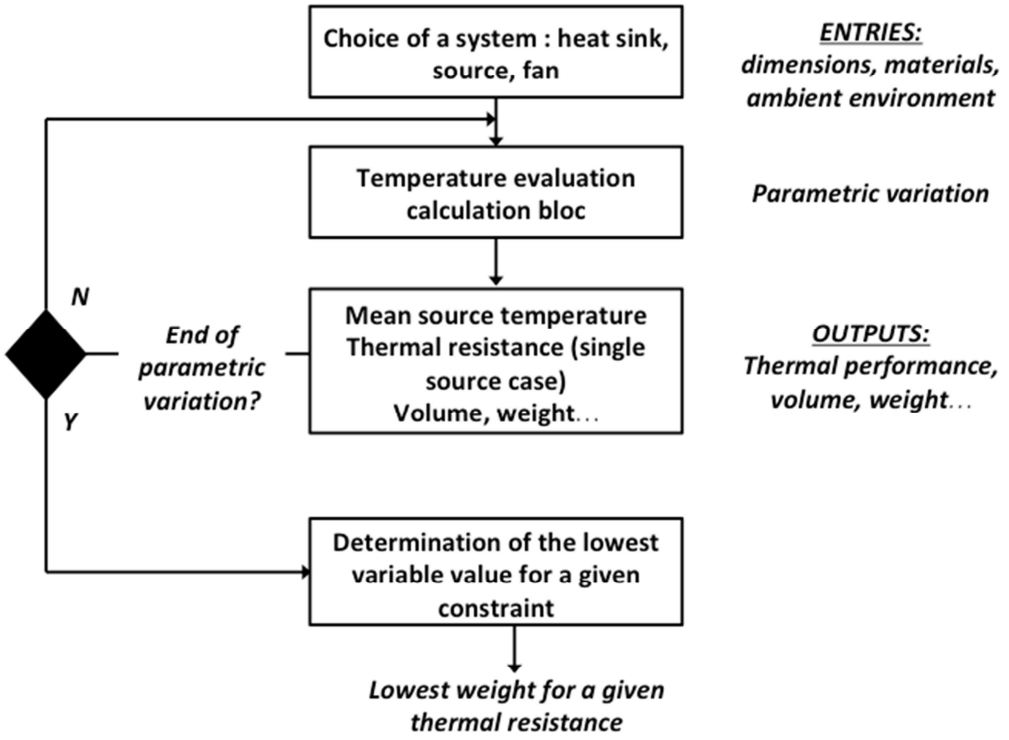

Fig. 9 : Optimization algorithm used to define the heat geometry with the lowest weight for a givent thermal resistance value.

The heat sink of Fig. 6 is used as a reference design for comparison, having a thermal resistance of 0.175K/W. Given the geometrical and mechanical constraints for the insertion of this heat sink in the real SiC converter, parameters were varied as presented in Table 1. The heat source is the same SiC module having 47mm width and 108mm length. The factor k, given by $k=n_{FIN}\cdot T_{FIN}/W$ gives an idea of the fin thickness $T_{FIN.}$

Parameters	Minimum value	Maximum value	Number of points
Base plate length (m)	0.108	0.150	5
Base plate width (m)	0.047	0.062	5
Base plate thickness (m)	0.003	0.020	9
Fin height (m)	0.01	0.08	9
Number of fins	10	40	31
$\boldsymbol{k=(n_{FIN}\cdot T_{FIN})/W}$	0.1	0.9	11

Table 1: Variation range and number of points for the variables defined for the optimization problem.

The calculation of 690525 options took 24 minutes and results of calculated points of thermal resistances and heat sink + fan weight are shown in Fig. 10, where the color of each point indicates the 5 values of base plate length explored. In this figure the Pareto front is also represented giving the minimal value of thermal resistance for each heat sink + fan weight.

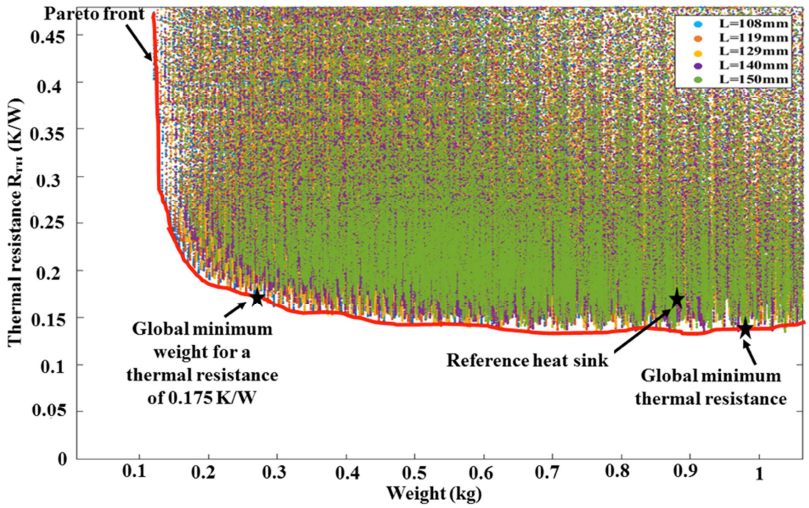

Fig. 10: Evolution of the global thermal resistance of the heat sink with the total weight for all the configurations explored during the calculation routine. The Pareto Front indicates the minimal thermal resistance for each weigth of the heat sink + fan. The optimal points obtained (minimum thermal resistance and minimum weight for the reference thermal resistance) as well as the reference heat sink are marked with a star.

With the optimization routine, the minimum thermal resistance of 0.1535K/W was found for a weight of 0.984kg (0.918kg the aluminum heat sink and 0.066kg the fan). Note that this optimal heat sink has about 12% less thermal resistance than that of the reference one but it is slightly heavier. This minimal thermal resistance point is marked in Fig. 9.

The point with minimum weight but with the same thermal resistance as the reference heat sink (0.175K/W) is marked in Fig. 10. Heat sink parameters associated to this point are given in Table 2 where the relative difference is given in (11).

$$\Delta x = \frac{\mathrm{x} - x_{ref}}{x_{ref}} \qquad (11)$$

where x is the value obtained by the optimization routine, and x_{ref} is the value related to the reference heat sink in Fig. 6.

Parameters	Value at the minimum point obtained	Relative difference Δx to reference heat sink (%)
Base plate length (m)	0.1080	-28%
Base plate width (m)	0.0620	0%
Base plate thickness (m)	0.0030	-71.4%
Fin height (m)	0.0450	-29.1%
Number of fins	38	+375%
$\boldsymbol{k=(n_{FIN}\cdot T_{FIN})/W}$	0.1800	-41.8%
Total weight (kg)	0.267	-70.2%
Thermal resistance (K/W)	0.174	-0.57%

Table 2:Values of the variables obtained after an optimization routine to find the configuration with the global minimum of weight for a given thermal resistance. Comparison with the reference heat sink on Fig. 6.

In order to give an example of the solutions obtained by the optimization routine, Fig. 11 presents the evolution of thermal resistance for different number of fins and different values of k. For that, 4 parameters were fixed at the optimal point given in Table 2 and variables n_{FIN} and k were varied. Curves related to the calculation of thermal resistance are shown in Fig. 11. Note that, for each different k (also each different fin thickness), there is an optimal number of fins which minimizes the thermal resistance. Obviously, the lower the number of fins, the

lower the weight for a given *k*. The point achieving minimum weight, at thermal resistance close to the reference one, as shown in Table 2, is marked in this graph and it corresponds to n_{FIN}=38 and *k*=0.18.

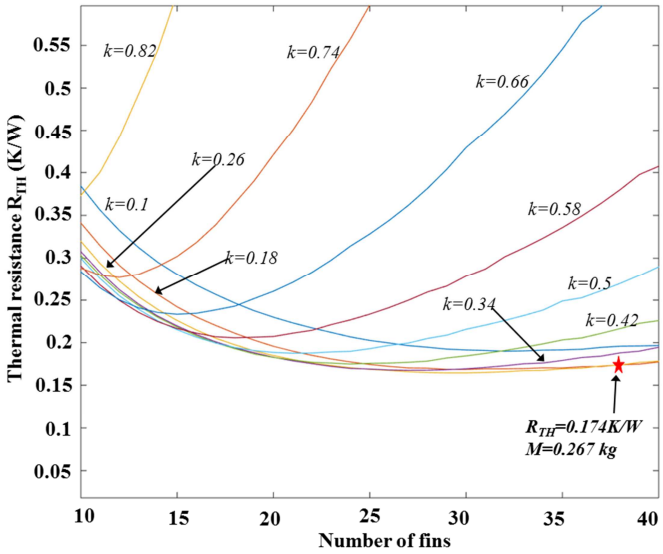

Fig. 11: Thermal resistance for different number of fins and fin thickness (expressed by the k *factor). In this example, the point corresponding to the minimum weight at the reference thermal resistance is marked with a star. Mass of this optimal heat sink is 0.267kg which is about 70% lower than the reference one.*

Note that although the number of points chosen for each variable is relatively low, the minimum weight for the thermal resistance of 0.175K/W found is 0.267kg, which is around 3.4 times lower than the weight of the reference heat sink. However, in order to find an even lower weight for the same thermal resistance, one could start another calculation with a parameter variation around the minimum point. For the example given here, the new minimum and maximum points for each variable are given in Table 3, and they are ± 10% away from the optimal point shown in Table 2. The minimum weight found by this new calculation is shown in Table 4.

Parameters	Minimum value	Maximum value	Number of points
Base plate length (m)	0.108	0.1188	6
Base plate width (m)	0.0558	0.062	6
Base plate thickness (m)	0.003	0.0033	6
Fin height (m)	0.0405	0.0495	11
Number of fins	34	40	6
$\boldsymbol{k=(n_{FIN}\cdot T_{FIN})/W}$	0.162	0.198	11

Table 3: Variation range and number of points for the variables defined for second optimization run.

Parameters	Final value	Relative difference Δx to the global minimum in Table 2	Relative difference Δx to reference heat sink
Base plate length (m)	0.108	0%	-28%
Base plate width (m)	0.062	0%	0%
Base plate thickness (m)	0.003	0%	-71.42%
Fin height (m)	0.0414	-8%	-34.8%
Number of fins	34	-10.5%	+325%
$k=(n_{FIN} \cdot T_{FIN})/W$	0.162	-10%	-47.7%
Total weight (kg)	0.241	-9.5%	-73%
Thermal resistance (K/W)	0.1747	+0.40%	-0.17%

Table 4: Values of the variables obtained after an optimization routine to find the configuration with the global minimum of weight for a given thermal resistance, after specification of the parameters variation range. Comparison with the reference heat sink on Fig. 6 and the optimal point in Table 2.

The choice of a systematic exploration gives interesting answers for the optimization of a heat sink weight. Several configurations have been explored, as the routine is very fast to execute. With a specific constraint (on the thermal resistance value), it has been possible to find the lowest weight configuration which reduces the heat sink weight of 73% when compared to the reference one. Besides the constraints defined in this example, other manufacturing criteria can be considered such as mechanical constraints or manufacturing cost constraints. The heat sink defined in the given example can be unrealistic regarding these criteria, but the optimization routine together with the model proposed in this paper enables us to explore all the configurations with several constraints and ensure a realistic and low weight heat sink.

The optimization results are summarized in Table 5.

	***Rth* (K/W)**	**Weight (kg)**
Optimization of *Rth*	0.1535	0.984
Optimization of weight	0.175	0.241
Reference heat sink	0.175	0.896

Table 5: Summary of results obtained after optimization of heat sink thermal resistance and weight.

6. CONCLUSION

Heat sink optimization is one of the most important aspects to take into account when reducing weight of power converters. Accurate 3D FEM simulations can be used but they are particularly time consuming and thus are hardly included in optimzation routines. Analytical models are fast but usually not enough accurate. For that reason, we developed an analytical modeling to calculate heat source mean temperature which is accurate and take into account heat spreading in the heat sink baseplate. This is particularly important when heat sources have a surface much smaller than that of the baseplate.

The developed model can also be used in problems with more than one heat source. In this manner, it calculates the average temperature of each heat source.

This analytical model was compared to precise 3D FEM simulation. Difference of no more than 2.5% was observed between results of analytical model and 3D FEM simulation. However, we observed an extreme gain on time using this analytical model. For a given heat sink geometry, calculation of thermal resistance took about 5.5ms using analytical model and about 15 minutes (about 160000 times slower) using a 3D FEM simulation.

The developed analytical model was used in a optimization routine in order to reduce the size of an existing performant heat sink + fan system. Optimization results show a reduction of about 12% on the thermal resistance if the objective is to reduce this value, or a reduction of 73% of the cooling system weight when compared to this commercial heat sink + fan system.

Development of such models can also be applied to other thermal problem such as thermal management of motors [15, 16] to get more precise analytical models. With this kind of analytical representation, and with a work on the geometry description, it could be possible to improve the existing analytical models dedicated to motors.

REFERENCES

[1] A. Castelan, B. Cougo, S. Dutour, T. Meynard, 3D Analytical modelling of heat sink distribution for fast optimization of power converters, Electrimacs 2017, Toulouse, France.

[2] R. E. Simons, Simple formula estimating thermal spread resistance, https://www.electronics-cooling.com/2004/05/simple-formulas-for-estimating-thermal-spreading-resistance/, accessed in January 2017

[3] S. Song, S. Lee, V. Au, Closed form equation for thermal constriction spreading resistance with variable boundary condition, https://www.researchgate.net/profile/Seaho_Song/publication/237713551_Closed-Form_Equation_for_with_Variable_Thermal_ConstrictionSpreading_Resistance_Boundary_Condition/links/55f17ec208aedecb69000bf7/Closed-Form-Equation-for-with-Variable-Thermal-Constriction-Spreading-Resistance-Boundary-Condition.pdf , accessed in January 2017.

[4] S. Song, S. Lee, V. Au, K. Moran, Constriction spreading resistance model for electronics packaging, https://pdfs.semanticscholar.org/62bc/d8050aaf0240a78e09e9ddd434ea7be88173.pdf, acessed in January 2017.

[5] U. Drofenik, A. Stupar, J. W. Kolar, Analysis of Theoretical Limits of Forced-Air Cooling Using Advanced Composite Materials with High Thermal Conductivity. *IEEE Transactions on Components, Packaging, and Manufacturing Technology*, Vol. 1, No. 4, pp. 528-535, April 2011.

[6] C. Gammeter, F. Krismer, J. W. Kolar, Weight Optimization of a Cooling System Composed of Fan and Extruded Fin Heat Sink. *IEEE Energy Conversion Congress and Exposition (ECCE USA 2013)*, Denver, Colorado, USA,September 15-19, 2013.

[7] M. M. Yovanovich, Y. S. Muzychka, J. R. Culham, Spreading resistance of isoflux rectangles and strips on compound flux channels. *Journal of thermophysics and heat transfer*, vol. 13, n o. 4, October-December 1999.

[8] M. M. Yovanovich, J. R. Culham and P. Teertstra, Analytical modeling of spreading resistance in flux tubes, half spaces, and compound disks. *IEEE Transactions on Components, Packaging, and Manufacturing Technology: Part A*, vol. 21, no. 1, pp. 168-176, Mar 1998.

[9] D. Guan, M. Marz, J. Liang, Analytical Solution of Thermal Spreading Resistance in Power Electronics. *IEEE Transactions on Components, Packaging and Manufacturing Technology*, 2(2), 278-285, 2012.

[10] M. J. M Krane, Constriction resistance in rectangular bodies. *Journal of Electronic Packaging*, 113(4), 392-396, 1991.

[11] M. M. Yovanovich, Y. S. Muzychka, J. R. Culham, Thermal spreading resistance of eccentric heat sources on rectangular flux channels. *Journal of Electronic packaging* 125.2 :178-185, 2003.

[12] A. Castelan, B. Cougo, J. Brandelero, D. Flumian, T. Meynard, Optimization of forced-air cooling system for accurate design of power converters. *IEEE 24th International Symposium on Industrial Electronics (ISIE)*, 367-372, 2015.

[13] P. Teertstra, M.M Yovanovich, J.R. Culham, T. Lemczyk, Analytical Forced convection modelling of plate fin heat sink, *15th IEEE SEMI-THERM symposium*, 1999.

[14] Estimating Parallel Plate-fin Heat Sink Pressure Drop , https://www.electronics-cooling.com/2003/05/estimating-parallel-plate-fin-heat-sink-pressure-drop/, accessed in July 2018[

15] G. Sooriyakumar, R. Perryman,, S. J. Dodds, Analyical thermal modelling for permanent magnet synchronous motors, *42nd International Universities Power Engineering Conference*, 2007

[16] D. Staton, D. Hawkins, M. Popescu, Thermal Behaviour of Electrical Motor- An Analytical Approach, https://www.motor-design.com/wp-content/uploads/2016/12/cwieme_2009_paper_mdl.pdf accessed in July 2018.

ACKNOWLEDGMENT:

Authors would like to thank partners of integration project, which are Airbus Operations, Airbus Group Innovations, Altran Technologies, Liebherr – Aerospace Toulouse, Safran Electrical & Power, Safran Electronics & Defense, Zodiac Aero Electric, Zodiac Actuations Systems and the French National Agency of Research (ANR).